# Fourier Transform measurements of SO2 absorption cross sections: I. Temperature dependence in the 24 000 – 29 000 cm–1 (345–420 nm) region

**ARTICLE** *in* JOURNAL OF QUANTITATIVE SPECTROSCOPY AND RADIATIVE TRANSFER · JANUARY 2009

Impact Factor: 2.65



**3 AUTHORS:**

Christian Hermans
Belgian Institute for Space Aeronomy
**119** PUBLICATIONS **1,754** CITATIONS
SEE PROFILE

A.C. Vandaele
Belgian Institute for Space Aeronomy
**214** PUBLICATIONS **4,639** CITATIONS
SEE PROFILE

Sophie Fally
Université Libre de Bruxelles
**62** PUBLICATIONS **3,397** CITATIONS
SEE PROFILE

Journal of Quantitative Spectroscopy & Radiative Transfer 110 (2009) 756–765

Contents lists available at ScienceDirect

Journal of Quantitative Spectroscopy & Radiative Transfer

journal homepage: www.elsevier.com/locate/jqsrt

# Fourier transform measurements of $SO_2$ absorption cross sections: I. Temperature dependence in the 24 000–29 000 $cm^{-1}$ (345–420 nm) region

C. Hermans [a], A.C. Vandaele [a,*], S. Fally [b,1]

[a] Belgian Institute for Space Aeronomy, 3 Av Circulaire, B-1180 Brussels, Belgium
[b] Université Libre de Bruxelles, Faculté des Sciences, Service de Chimie Quantique et Photophysique, C.P. 160/09, 50 Avenue F.D. Roosevelt, B-1050 Brussels, Belgium

ARTICLE INFO

*Article history:*
Received 24 November 2008
Received in revised form
29 January 2009
Accepted 30 January 2009

*Keywords:*
Laboratory measurement
Absorption cross section
Fourier transform spectroscopy
Sulfur dioxide

ABSTRACT

Absorption cross sections of $SO_2$ have been obtained in the 24 000–29 000 $cm^{-1}$ spectral range (345–420 nm) with a Fourier transform spectrometer at a resolution of 2 $cm^{-1}$. Pure $SO_2$ samples were used and measurements were performed at room temperature (298 K) as well as at 318, 338 and 358 K. This is the first time that temperature effects in this spectral region are reported and investigated. This paper is the first of a series that will report on measurements of the absorption cross section of $SO_2$ in the UV/visible region at a higher than previously reported resolution and that will investigate temperature effects in support of tropospheric, stratospheric and astrophysical or planetary applications.



## 1. Introduction

Sulfur dioxide ($SO_2$) is an important constituent on Venus [1–5] and Io [6–9], where it actively participates to the photochemistry of their atmospheres. It has also been observed in comets [10–13]. $SO_2$ is a trace species in the Earth's atmosphere, mainly present in the troposphere [14–16], where it is a primary pollutant emitted by fuel combustion. The most important natural sources of $SO_2$ are the oxidation of sulfur compounds from oceans and marshes and from volcanic eruptions and outgassing. Most volcanic $SO_2$ emissions remain in the troposphere, where the lifetime of the species strongly depends on the meteorological conditions. $SO_2$ is also present in the stratosphere [17,18] in high concentrations, but only after major volcano eruptions. Measurements of $SO_2$ have recently been performed from satellites, either for monitoring volcanic eruptions [19–24], or to observe tropospheric content [25]. Measurements using satellite instruments are generally based on the spectroscopic signature of $SO_2$ in the UV/visible region.

$SO_2$ presents three main regions of absorption in the near ultraviolet domain. The strongest band lies in the 45 000 $cm^{-1}$ (220 nm) region and corresponds to the $\hat{C}^1B_2$–$X^1A_1$ electronic transition. Between 29 000 and 40 000 $cm^{-1}$ (250–345 nm) extends a medium absorption structure, which can be ascribed to at least two electronic transitions. Underlying the structured bands of the $A^1A_2$–$X^1A_1$ [26], the 'continuous' absorption has been attributed to the $B^1B_1$–$X^1A_1$ transition, which was predicted by theory [27] and measured by Brand et al. [28]. The $A^1A_2$–$X^1A_1$ transition is forbidden but is observed because of strong vibrational interactions through the $\nu_3$ vibration mode and is strongly perturbed by the $^1B_1$ state. The

* Corresponding author.
*E-mail address:* a-c.vandaele@aeronomie.be (A.C. Vandaele).
[1] Now at BISA.

0022-4073/$ - see front matter © 2009 Elsevier Ltd. All rights reserved.
doi:10.1016/j.jqsrt.2009.01.031

allowed transition $B^1B_1$–$X^1A_1$ is so perturbed that no rotational or vibrational analysis is possible. It forms a continuum due to the density of weak absorptions. A weak absorption feature arises in the 24 000–29 000 $cm^{-1}$ region (345–420 nm). It has been assigned to the $a^3B_1$–$X^1A_1$ electronic transition and is a spin-forbidden transition. Several vibrational assignments of the triplet system have previously been given [29–33]. Joens [34] proposed two different assignments of the vibrational structures based on nine bands reported by Brand et al. [29,30] and eight additional bands observed by Baskin et al. [35]. They advocated for new measurements to determine the correct assignments. Recently, Huang et al. [36] analyzed the rotational structure of two bands of the $a^3B_1$–$X^1A_1$ transition using laser-induced excitation in a supersonic jet. They confirmed the assignment of the (0 1 0) and (1 0 0) vibrational levels, and determined their band origins for transitions originating from the ground level of the $^1A_1$ state.

The present paper is the first of the series reporting results of a study that has investigated the temperature effect on the $SO_2$ absorption cross section in the 24 000–44 500 $cm^{-1}$ spectral region, covering thus two of the UV absorption features of $SO_2$. This first paper deals with the 24 000–29 000 $cm^{-1}$ region corresponding to the $a^3B_1$–$X^1A_1$ electronic transition, while a second paper will be devoted to the measurements of the absorption cross section in the 29 000–44 500 $cm^{-1}$, much used in atmospheric remote sensing. The aim of the present work is to provide absorption cross sections at a higher than previously reported resolution and to investigate high temperature effects in support of tropospheric, stratospheric and astrophysical or planetary applications.

## 2. Experimental description

Measurements of the absorption cross sections of gaseous $SO_2$ have been performed at the resolution of 2 $cm^{-1}$ (maximum optical path difference = 0.45 cm) which corresponds to 0.032 nm at 400 nm over the 24 000–29 000 $cm^{-1}$ (345–420 nm) spectral range under different pressure and temperature conditions with pure samples of $SO_2$. All measurements have been carried out with a Fourier transform spectrometer BRUKER IFS120 M in combination either with a Xenon high pressure lamp (150 W) or a Tungsten lamp (250 W), and with a GaP diode as detector (see Fig. 1). The different combinations of lamps-detector allowed the recordings in two different spectral region: (i) W-GaP: from 23 500 to 30 750 $cm^{-1}$ and (ii) Xe–GaP: from 25 000 to 32 000 $cm^{-1}$. A short-pass filter (Melles Griot, 50% cutoff at 450 nm) was also used. A 200 cm long cell was used during this study. The cell is made of stainless steel and is fitted with quartz windows. It can be temperature stabilized either by cooling it down by the circulation of a fluid around it, or by heating it by the use of a heating coil. Five temperature sensors are evenly distributed inside the cell and give information on the temperature distribution and evolution inside it. Pressure was measured by temperature stabilized Baratron capacitance gauge (1000 and 10 Torr full scale) characterized by a 0.03% reading error.

$SO_2$ samples (Indugas, >99.98% stated purity) were used without further purification. One complete experiment at a given temperature consisted of: (i) a blank measurement (cell empty), (ii) measurements with the pure gas at several increasing or decreasing pressures, and finally (iii) a blank measurement. Such a procedure was repeated at least two times for each temperature. Spectra were recorded at 298, 318, 338, and 358 K, in single-sided mode during the forward and backward movement of the mobile mirror with boxcar apodization. Depending on the experimental conditions, a certain number of mirror scans (interferograms) were averaged to get an acceptable signal to noise. This number of scans was recorded in several blocks that were averaged at the end to obtain the spectrum. Recording using successive blocks offered the possibility to follow the pressure inside the cell and was also used to monitor any change of absorption from one block to the other. The experimental conditions are summarized in Table 1.

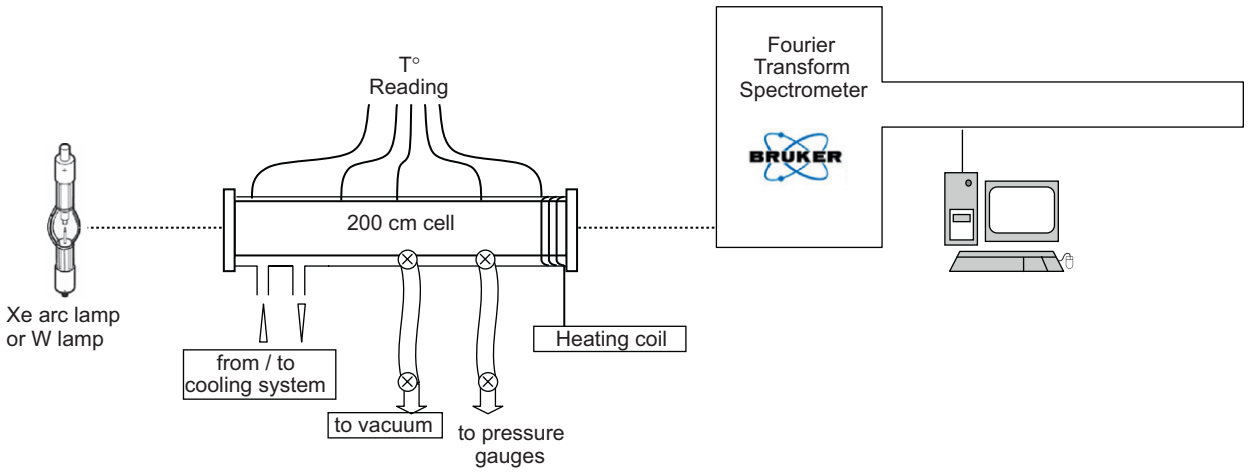


**Fig. 1.** Experimental setup.

**Table 1**
Experimental description: for each temperature and each lamp–detector combination, the number of different pressures is indicated, as well as the pressure range investigated and the recording characteristics.

| $T$ (K) | Lamp–detector | No. of diff. pressures | Pressure range (Torr) | No. of co-added scans[a] |
|---|---|---|---|---|
| 298 | W–GaP | 10 | 31–130 | $40 \times 128$ |
| | Xe–GaP | 5 | 0.4–66.2 | $40 \times 128$ |
| 318 | W–GaP | 11 | 31–150 | $40 \times 128$ |
| | Xe–GaP | 5 | 0.4–63.7 | $40 \times 128$ |
| 338 | W–GaP | 14 | 20–175 | $40 \times 128$ |
| | Xe–GaP | 5 | 0.5–68.4 | $40 \times 128$ |
| 358 | W–GaP | 15 | 30–265 | $40 \times 128$ |
| | Xe–GaP | 5 | 0.6–73.0 | $40 \times 128$ |

[a] The total number of co-added scans is the results of the co-addition of all the scans performed in the several successive blocks: $40 \times 128$ means that 40 blocks of spectra were recorded successively, and each of these blocks consisted of 128 scans of the mobile mirror of the spectrometer.

## 3. Results

Absorption cross sections were deduced using the following equation:

$$\sigma(\nu) = \frac{1}{n_{SO_2} d} \times \ln\left(\frac{(I_{0,\ before}(\nu) + I_{0,\ after}(\nu))/2}{I(\nu)}\right) \quad (1)$$

where $n_{SO_2}$ is the concentration of $SO_2$ inside the cell calculated from the pressure measurement, $d$ is the cell length (207.2 cm), $I_{0,\ before}$ and $I_{0,\ after}$ are, respectively, the blank spectra recorded before and after the $SO_2$ measurement, and $I$ is the intensity measured when the cell contained the species under investigation.

Fig. 2 shows the absorption cross section of $SO_2$ obtained at room temperature. It also illustrates that the final cross section is the result of averaging all available data on optimized spectral regions. In the case of the room temperature measurements, a total of 15 individual cross sections were obtained corresponding to different $SO_2$ pressures. Each of these cross sections was only considered on a restricted wavenumber interval to optimize the ($n_{SO_2} \times d$) optical density and minimize noise level. No pressure dependence could be observed in those individual cross sections. Finally all available data corresponding to a given wavenumber were averaged. The number of averaged data is shown in the bottom Panel of Fig. 2. It varies between 1 and 12 depending on the wavenumber. It is maximum between 26 000 and 27 000 $cm^{-1}$ which is covered by most of the spectra recorded with the two different lamp-detector combinations. The standard deviation of all the considered measurements is also given. It is lower than $0.13 \times 10^{22}$ $cm^2$/molecules. This corresponds to a standard deviation of about 1.5% at the maximum, which is in-between the error and rms error stated in this work (see next section). Very similar values were obtained for the absorption cross section at the higher temperatures.

### 3.1. Uncertainties

The uncertainties of the absorption cross sections have been estimated by considering the different error sources: Concentration, uncertainties due to temperature error (2 K, including the reading error, stabilization in time and along the cell), pressure (3%), and length of the cell (0.25%). Taking into account all these error sources, the total systematic uncertainty on the cross section has been estimated to be of the order of 4%, from a simple error propagation calculation.

Non-systematic uncertainties on the absorption cross sections were also estimated. Those mostly are due to the noise level on the absorbance (i.e. the noise levels on $I$ and $I_0$) and to the lamp drift with time. Noise levels were evaluated as the rms standard deviation of the measured spectra where no absorption features are located. Lamp drift was estimated by looking at the evolution of the intensity of the lamp spectra where there is no absorption by $SO_2$. This assumes that the evolution of the lamp spectrum in time does not vary with wavenumbers. It was found that the intensity variation was of the order of 1% for the W lamp and 3% for the Xe lamp. The uncertainties on the measurements performed at the higher temperatures are somewhat better, because, as stated in Table 1, the number of different spectra is larger. In the case of the measurements at 358 K, up to 19 individual cross sections have been averaged. Non-systematic errors are given in the data files, which are available from the website of the Belgian Institute for Space Aeronomy (http://www.aeronomie.be/spectrolab/).

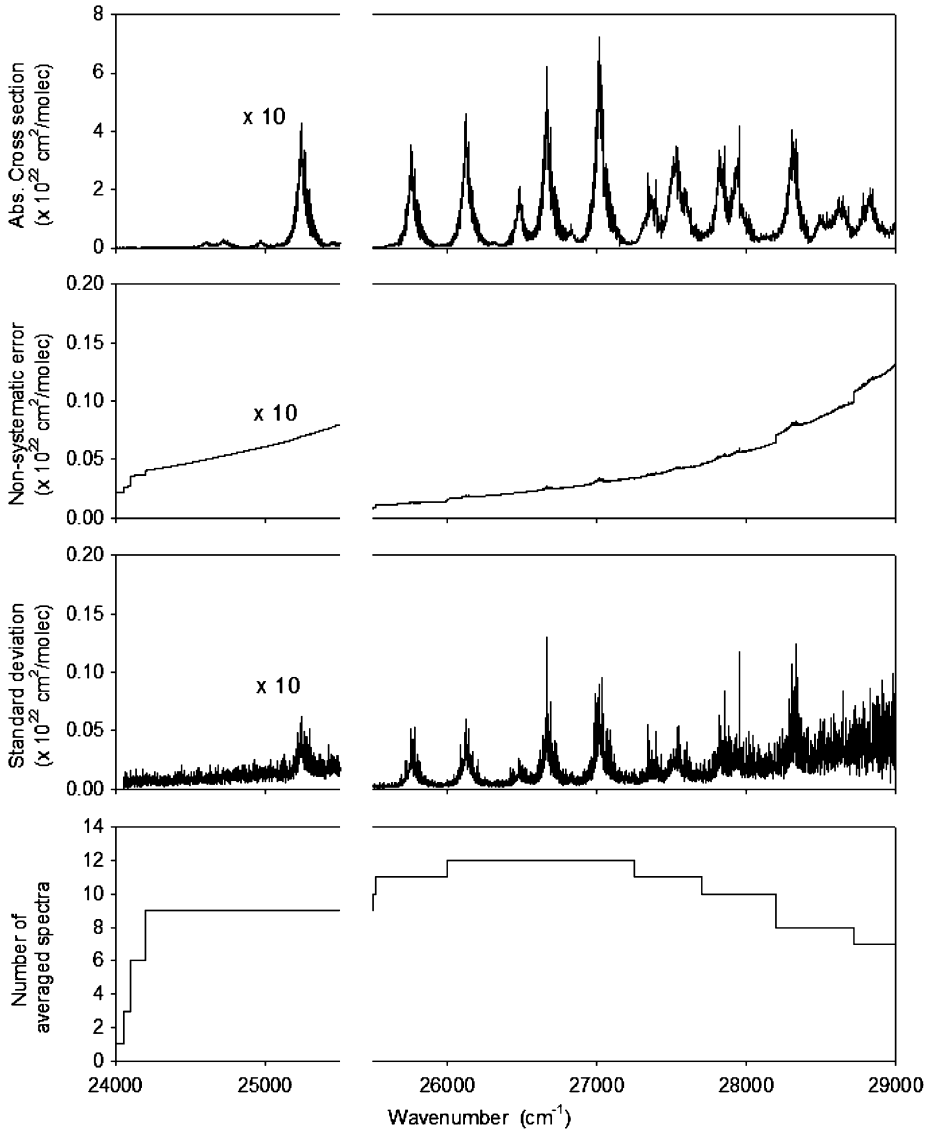


**Fig. 2.** Absorption cross sections of $SO_2$ at 298 K (top panel). The non-systematic error and the standard deviation of the measurements are also given, as well as the number of averaged spectra. The standard deviation represents the experimental variability of the cross section.

The wavenumber calibration has been performed using 37 lines of $I_2$, whose positions were taken from the Iodine atlas of Gerstenkorn and Luc [37,38]. Spectra of $I_2$ were recorded at the resolution of 0.042 $cm^{-1}$ with the same instrument that was used for the measurements of $SO_2$. The estimated accuracy on the wavenumbers is of the order of 0.02 $cm^{-1}$, which represents the average value of the shifts observed between the positions obtained in this work and those of the atlas. Note that the positions of the atlas were first corrected to correspond to air wavenumbers using the Edlen formula [39], as the spectrometer was not operated under vacuum. Therefore, all wavenumbers given in this work are expressed in air and are defined as $1/\lambda_{air}$.

### 3.2. Assignment of the vibronic structures

Several assignments of the triplet system $a^3B_1$ have already been proposed [29–33]. More recently, Joens [34] combined measurements from Brand et al. [29,30] and from Baskin et al. [35] to determine two possible assignments. Given the resolution of the present work, band centers cannot be determined with great accuracy. However, the positions of the most prominent band heads can be evaluated. Some of them, corresponding to bands assigned by Joens [34], are given in Table 2. Note that the band heads positions have been converted to vacuum wavenumbers in this table. As discussed in [30,34], the

**Table 2**
Assignment of the vibrational structures.

| Band heads[a] | Assignment 1[b] | | Assignment 2[b] | |
|---|---|---|---|---|
| Obs ($cm^{-1}$) | Vib level | Obs−calc[c] ($cm^{-1}$) | Vib level | Obs−calc[c] ($cm^{-1}$) |
| 25774.695 | 0 0 0 | 0.4 | 0 0 0 | 0.5 |
| 26135.584 | 0 1 0 | 2.7 | 0 1 0 | 1.2 |
| 26492.974 | 0 2 0 | 2.0 | 0 2 0 | 1.2 |
| 26680.916 | 1 0 0 | −0.5 | 1 0 0 | 1.7 |
| 27031.807 | 1 1 0 | −3.9 | 1 1 0 | −1.6 |
| 27385.197 | 1 2 0 | −16.2 | 1 2 0 | −11.5 |
| 27527.653 | 2 0 0 | 1.6 | 0 0 2 | −6.0 |
| 27619.624 | 0 0 2 | 0.1 | 2 0 0 | −19.1 |
| 27843.054 | 2 1 0 | 17.9 | 0 1 2 | 8.9 |
| 27944.023 | 0 1 2 | −2.0 | 2 1 0 | −9.8 |
| 28327.902 | 3 0 0 | −6.6 | 1 0 2 | −3.7 |
| 28507.346 | 2 3 0 | −2.1 | 0 3 2 | −7.3 |
| 28532.338 | 1 0 2 | −1.3 | 3 0 0 | −3.3 |
| 28637.805 | 3 1 0 | −0.4 | 1 1 2 | 2.8 |
| 28675.293 | 1 6 0 | −6.1 | – | – |
| 28839.741 | 1 1 2 | −2.0 | 3 1 0 | 9.2 |
| 29057.672 | 4 0 0 | −0.8 | – | – |
| 29109.156 | – | – | 2 0 2 | 28.2 |
| Rms[d] | | 6.7 | | 10.6 |

[a] Vacuum wavenumbers.
[b] Assignments given in [34]: Assignment 1 is based on the assignment proposed by Baskin et al. [35] and Assignment 2 is a new assignment proposed by Joens [34].
[c] Difference between the observed and calculated positions of the band heads. The calculated positions were determined using two different sets of the vibrational constants deduced from the two different assignments [34].
[d] Root mean square of the Obs−calc differences.

band heads appear typically 8 $cm^{-1}$ higher in energy than the band origins. Using the vibrational constants of the $^3B_1$ state and the assignments of the vibrational structures given in [34], we have compared the calculated positions of the band centers to the band heads found in this work taking into account the 8 $cm^{-1}$ shift. Results of this comparison are shown in Table 2, for the two assignments proposed by Joens [34]. It can be seen that none of the assignment is satisfactory, the root mean square of the difference being, respectively, 6.7 and 10.6, with some large difference values in both schemes. Based solely on these selected band measurements, we cannot easily help discriminating between the two different assignments proposed by Joens [34]. The complete assignment of all the bands observed in the present work is under progress. However, this is not an easy task, as the rotational structure is blended at the resolution used in this work, preventing the precise determination of the band centers. A more accurate investigation of the $a^3B_1$–$X^1A_1$ transition has been initiated by recording spectra at a higher resolution (0.042 $cm^{-1}$).

### 3.3. Temperature effect

The temperature effect was investigated by measuring the absorption cross sections at different temperatures (298, 318, 338, and 358 K). Fig. 3 illustrates this effect and shows that two opposite trends are observed depending on the spectral region: Around each peak and at higher wavenumbers, intensities increase when temperature decreases, whereas at wavenumbers lower than the maxima, they decrease.

The temperature effect was investigated by considering a linear dependency with respect to temperature, defining a temperature coefficient $c(\nu)$.

$$\sigma_T(\nu) = \sigma_{298\,K}(\nu) + c(\nu)(T - 298) \quad (2)$$

The choice to use this simple description for the temperature effect results from the small number of different temperatures investigated in this work, but also from a detailed analysis of the evolution of the absorption cross section with temperature. The linearity of the temperature dependence is illustrated in Fig. 4 for a series of selected wavenumbers, corresponding to wavenumbers lower than maxima (left panel) and to wavenumbers around the peaks and higher (right panel). Moreover, this choice was motivated by the simplicity and usefulness of such a model and by our previous findings and experience with $NO_2$ [40,41].

The $c(\nu)$ coefficient was obtained by least squares fitting of the absorption cross sections at the different temperatures and at a given wavenumber $\nu$ with the expression in Eq. (2), weighting as $1/\varepsilon^2$, where $\varepsilon$ is the experimental error (systematic and non-systematic) on the measured values. The spectral variation of the temperature parameter is shown in Fig. 5. It is the strongest and negative at the peaks of absorption whereas it is null or slightly positive elsewhere. The different behavior of the temperature dependency is also shown in the bottom panel of Fig. 5, where the correlation

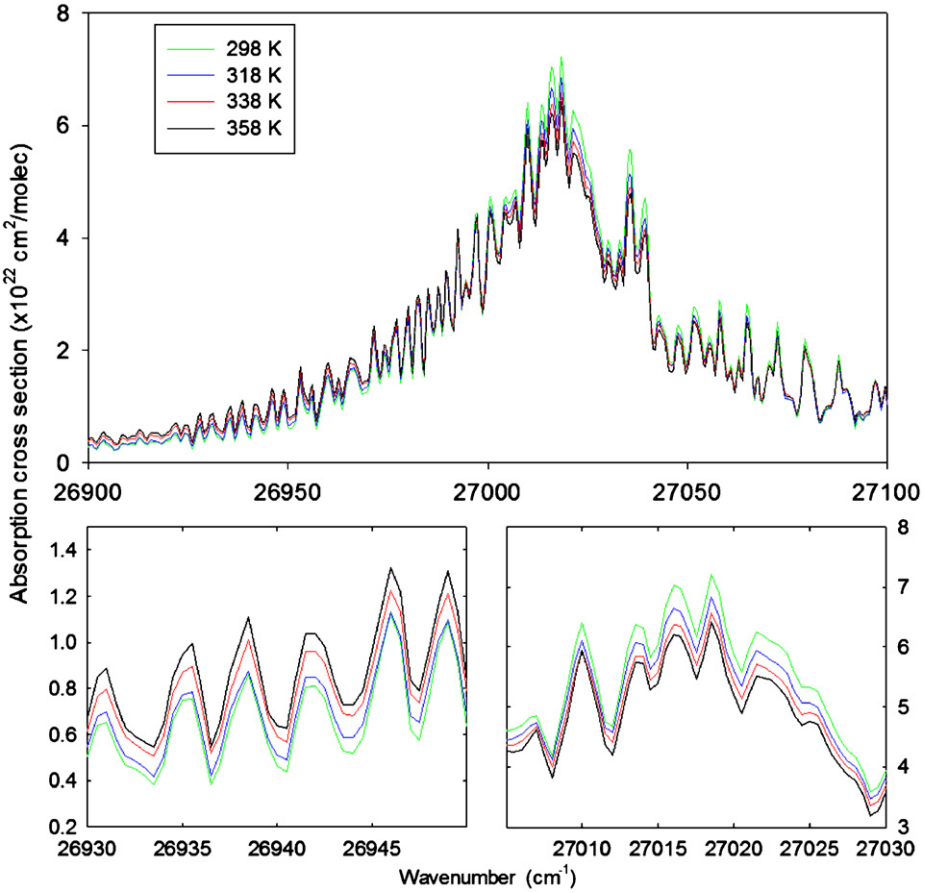


**Fig. 3.** Evolution of the $SO_2$ absorption cross section with temperature: 298 K (green), 318 K (blue), 338 K (red), and 358 K (black). The two bottom panels are zoomed regions of the top panel, showing different temperature dependence. For interpretation of the references to color in this figure legend, the reader is referred to the web version of this article.

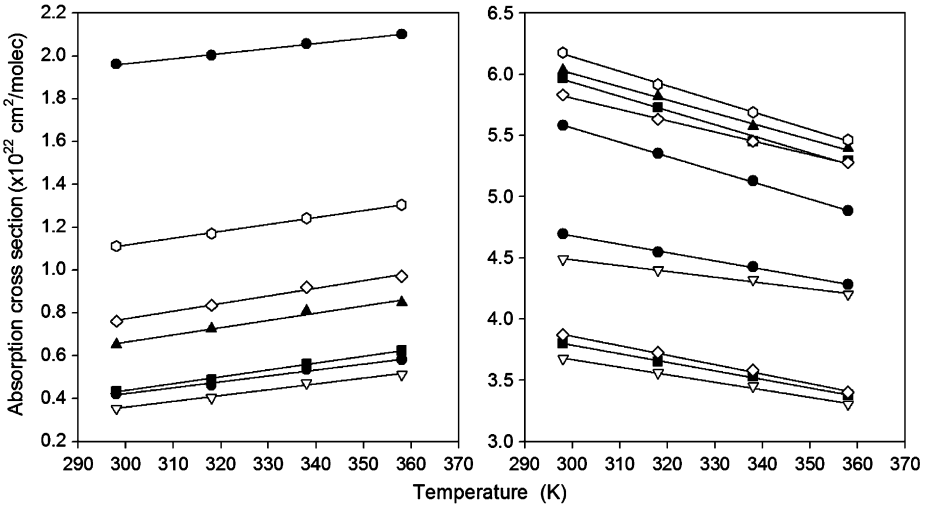


**Fig. 4.** Linearity of the temperature dependence of the $SO_2$ absorption cross section in the temperature range investigated in this study. On the left panel: evolution of intensities for wavenumbers lower than the maximum (between 26 912.5 and 26 974.0 cm$^{-1}$). On the right panel: evolution of the intensities at the peak and for higher wavenumbers (between 27 006.0 and 27 038.0 cm$^{-1}$).

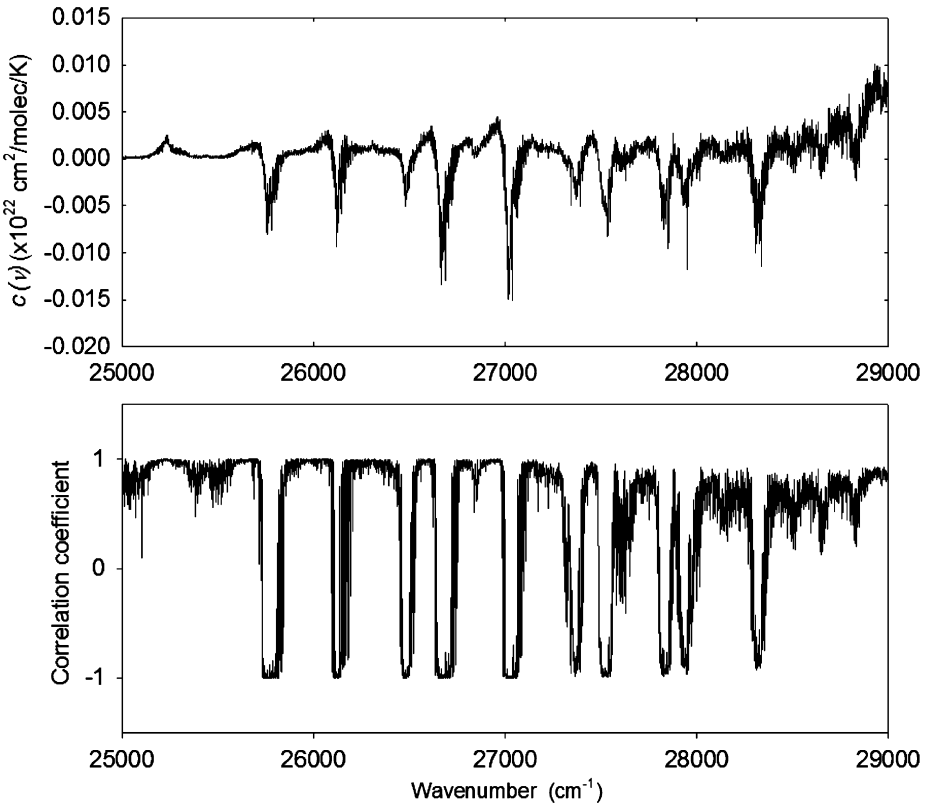


**Fig. 5.** Temperature dependence of the $SO_2$ absorption cross section: (a) temperature coefficient and (b) correlation coefficient of the linear regression.

**Table 3**
Description of existing data in the literature.

| Author | $T$ (K) | Spectral region (nm) | Technique[a] | Resolution[b] | Wavelength sampling | $\varepsilon_{wn}$ | $\varepsilon_{xs}$ (%) | Comment |
|---|---|---|---|---|---|---|---|---|
| Sidebottom et al. [42] | 298 | 337.5–403.0 | $n^c$ | $n^c$ | $n^c$ | $n^c$ | $n^c$ | Data only from graph |
| Manatt and Lane [43] | 293 | 106–403 | $n^c$ | 0.1 nm (6 $cm^{-1}$) | 0.1 nm | 0.1 nm | 1 | Compilation of literature data based on Sidebottom data in the 337–403 nm region |
| Sprague and Joens [45] | 298 | 345–406 | *D*/*W*+*M* | 0.1 nm (6 $cm^{-1}$) | 0.04 nm | 0.05 nm | 1 | Only intensity at peaks data from graph |

For each reference, the following information is given: temperature of the recording, spectral region investigated, technique used, spectral resolution, wavelength sampling, uncertainty $\varepsilon$ on the wavelength scale and on the cross section, and some general comment.
[a] *D*—deuterium lamp; *W*—tungsten lamp; *M*—monochromator.
[b] Conversion to wavenumber ($cm^{-1}$) performed at 25 000 $cm^{-1}$.
[c] Not given.

coefficient of the linear regression is plotted. This coefficient is defined as

$$r = \frac{\sum xy}{\sqrt{(\sum x^2)(\sum y^2)}} \tag{3}$$

where $x$ are the independent variables an $y$ the dependent ones. It is equal to 1 (perfect linear regression with positive slope) for wavenumber lower than the peak maxima, and −1 (perfect linear regression with negative slope) at the peaks and higher wavenumbers.

## 4. Comparison with data from the literature

Compared to $SO_2$ absorption cross sections measurements in the 30 000–40 000 $cm^{-1}$ region, measurements below 29 000 $cm^{-1}$ are very scarce. Table 3 summarizes the experimental conditions of the existing literature data. Sidebottom et al. [42]

discussed the photooxidation of $SO_2$ and reported plots of the extinction coefficient of $SO_2$ in the 340–400 nm region. Manatt and Lane [43], who did a compilation of absorption cross sections existing in the literature, have digitalized the data of Sidebottom et al. [42] from the figures in their paper. These data were the only ones considered in this spectral region. However, Manatt and Lane [43] introduced some modifications to the data: (i) by shifting them by 0.67 nm to the red after comparison with peak positions from measurements performed by Clements [44]; (ii) by correcting for the sinking baseline at the short wavelength side of the Sidebottom et al. data. Finally data were computed at 0.1 nm intervals. Sprague and Joens [45] report measurements of $SO_2$ in the 320–405 nm region at a temperature of 298 K and a resolution of 0.1 nm. Vandaele et al. [46] report measurements of the $SO_2$ absorption cross sections from 27 000 $cm^{-1}$. However, the range of $SO_2$ partial pressures investigated in that work was not adequate to measure any $SO_2$ absorption below 30 000 $cm^{-1}$. All the measurements reported in the literature have been performed at room temperature. Absorption cross sections at the higher temperatures presented in this paper have, to our knowledge, never been reported before.

One major problem arising when comparing data sets, is how to take accurately into account the different resolutions at which the spectra were recorded. Another problem encountered with most of the data obtained with conventional grating instruments is their poor wavelength calibration. In general, a shift as well as a stretching of the scale should be introduced. In this study we have, however, limited the correction of the wavelength scale of the different literature data sets to a shift because it keeps the frequency spacing constant, and the introduction of a stretch would not change the conclusions of the comparison. The use of a FTS greatly improves the accuracy on the determination of the wavenumber scale, because the calibration of interferometers is very accurate and stable (Connes advantage). In order to perform reliable comparisons between absorption cross-sections obtained at different resolutions, the data of the present work have been convolved with a Gaussian function to correspond to the resolutions of the literature data.

The detailed comparison of the data obtained in this work with data of the literature is presented in Fig. 6, where the absolute differences are shown in the lower panels. In those comparisons, shifts have already been applied so that some conclusions on the amplitude of the cross sections can be drawn. Results of the systematic comparison between the literature data and the data from the present study are summarized in Table 4. Each data set from the literature has been fitted by the linear expression

$$\sigma_{Lit}(\lambda + shift) = a + b \times \sigma_{this\ work}(\lambda + convolution) \tag{4}$$

where the parameter $a$ and $b$ represents the offset and a multiplicative factor. For comparison purposes the shifts have also been converted to nanometers (conversion performed at the center of each spectral interval considered). They must be compared to the given accuracies for the wavelength scales of the literature data. The comparison of data has been first performed on the largest possible spectral interval (25 600–28 100 $cm^{-1}$) and then on smaller intervals encompassing only one absorption feature. This allowed us to draw better conclusions on the homogeneity of the different data sets.

Manatt and Lane [43] state an accuracy on their wavelength scale of 0.1 nm. However, they reported inconsistencies between different data sets in the 337–403 nm region on which they based their compilation. Sidebottom et al. data [42] were shifted by 6.7 nm to better correspond to the peak position reported by Clements [44], but the correspondence was not perfect and varied with wavelength (see Fig. 2 in their paper). Moreover, they found differences between two data sets

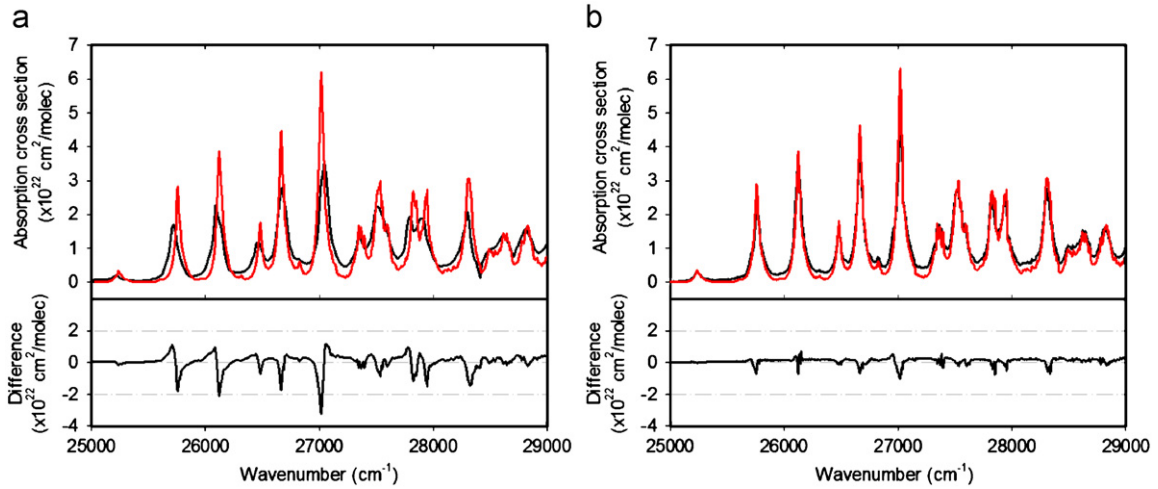


**Fig. 6.** Comparison of the $SO_2$ absorption cross section at 298 K of this work (red) with data from the literature (black): (a) Manatt and Lane [43], shifted by −41.7 $cm^{-1}$ and (b) Sprague and Joens [45], shifted by 5.9 $cm^{-1}$. The bottom panels show the $\sigma_{Lit}-\sigma_{This\ work}$ differences. For interpretation of the references to color in this figure legend, the reader is referred to the web version of this article.

**Table 4**
Results of the comparison of the $SO_2$ absorption cross sections at room temperature with data from the literature.

| Reference | $\sigma_{Lit} = a + b \times \sigma_{This\ work}$ | | Shift | |
|---|---|---|---|---|
| | $a$ ($cm^2$/molecules) | $b$ | ($cm^{-1}$) | (nm) |
| *Manatt and Lane* [43] (*resolution* = 0.1 *nm*) | | | | |
| [25 600–28 100] | 4.90e−023 | 0.56 | −41.7 | −0.58 |
| [25 850–26 300] | 2.54e−023 | 0.66 | −68.0 | −1.00 |
| [26 300–26 800] | 4.76e−023 | 0.63 | −38.3 | −0.54 |
| [26 800–27 200] | 5.09e−023 | 0.62 | −17.7 | −0.24 |
| [27 200–27 700] | 4.33e−023 | 0.69 | −49.6 | −0.66 |
| [27 700–28 100] | 5.95e−023 | 0.54 | −76.6 | −0.99 |
| *Manatt and Lane* [43] (*resolution* = 1.0 *nm*) | | | | |
| [25 600–28 100] | 2.61e−023 | 0.79 | −42.1 | −0.58 |
| [25 850–26 300] | 9.22e−024 | 0.87 | −66.8 | −0.99 |
| [26 300–26 800] | 2.36e−023 | 0.88 | −38.5 | −0.55 |
| [26 800–27 200] | 2.01e−023 | 0.85 | −17.8 | −0.24 |
| [27 200–27 700] | 2.08e−023 | 0.89 | −48.2 | −0.64 |
| [27 700–28 100] | 2.20e−023 | 0.82 | −73.2 | −0.94 |
| *Sprague and Joens* [45] (*resolution* = 0.1 *nm*) | | | | |
| [25 600–28 100] | 2.61e−023 | 0.84 | 5.9 | 0.08 |
| [25 600–25 850] | 1.95e−023 | 0.81 | 10.3 | 0.16 |
| [25 850–26 300] | 1.96e−023 | 0.96 | 6.7 | 0.10 |
| [26 300–26 800] | 2.35e−023 | 0.83 | 5.3 | 0.08 |
| [26 800–27 200] | 3.50e−023 | 0.80 | 6.4 | 0.09 |
| [27 200–27 700] | 2.88e−023 | 0.87 | 2.5 | 0.03 |
| [27 700–28 100] | 3.17e−023 | 0.80 | 2.7 | 0.03 |

$a$ and $b$ represent the offset and the multiplicative factor existing between the values of this work and the literature data. The last column indicates the wavenumber shift $\nu_{Lit} - \nu_{This\ work}$, expressed in wavenumber and wavelength (at the center of the spectral interval).

from Sidebottom et al. [42,47]. The conclusions of our study are similar: There is still a shift, and it is not constant over the whole interval (see Fig. 6a). The Manatt and Lane [43] data are systematically lower in intensity at the peak of absorption, and higher in-between, with a mean value of the difference being $0.05 \times 10^{22}$ $cm^2$/molecules (standard deviation = $0.5 \times 10^{22}$ $cm^2$/molecules). Sidebottom et al. [42] do not give any indication on the resolution they used to record their spectra and Manatt and Lane [43] did not correct for this: They just interpolated the data on a 0.1 nm grid scale. However, we have found that our data convolved at 0.1 nm still presented higher and finer structures than those in the Manatt and Lane data. We have done a similar comparison after convolution of our data by a Gaussian of 1.0 nm width. In this case the resolutions of the two data sets seem more similar. The results of this comparison are also given in Table 4, and indicate a better agreement with respect to the intensities of the structures. Sprague and Joens [45] give a wavelength accuracy of the order of 0.05 nm, with a sampling of 0.04 nm and a resolution of 0.1 nm. Our comparison shows that the shift between their data and ours varies from 0.03 to 0.1 nm. The comparison shows that there is a clear offset in the absolute values of the intensity of the absorption cross sections and that the intensities of Sprague and Joens are systematically lower at the peaks of absorption. The mean value of the difference is $0.09 \times 10^{22}$ $cm^2$/molecules, with a standard deviation of $0.2 \times 10^{22}$ $cm^2$/molecules.

## 5. Conclusions

The paper presents new absorption cross sections of $SO_2$ at the resolution of 2 $cm^{-1}$ as well as their temperature dependence in the 24 000–29 000 $cm^{-1}$ (345–420 nm) spectral region. The lack of homogeneous, accurate and high-resolution literature data in this region prompted the new measurements reported in this study. This is also the first time that temperature effects have been investigated in this region.

It has been shown that the existing assignments for some of the vibrational structures observed in this work are not satisfactory. This would require further investigation and probably new measurements at higher resolution. Such measurements are planned in the near future.

The complete data set comprising the absorption cross sections at different temperatures is available in electronic format from the website of the Belgian Institute for Space Aeronomy: http://www.aeronomie.be/spectrolab/.

## Acknowledgments

This project was supported by the National Fund for Scientific Research (FNRS FRFC convention no. 2.4542.08), by the Belgian Federal Science Policy Office (SSD Program) and by the Communauté Française de Belgique (Actions de Recherche Concertées).

## References

[1] Belayev D, Fedorova A, Korablev O, Vandaele AC, Mahieux A, Neefs E, et al. $SO_2$ detection in the Venus mesosphere with the SOIR spectrometer on board Venus Express. J Geophys Res 2008;113(E00B25), doi:10.1029/2008JE003143.
[2] Bertaux J-L, Widemann T, Hauchecorne A, Moroz VI, Ekonomov AP. VEGA 1 and VEGA 2 entry probes: an investigation of local UV absorption (220–400 nm) in the atmosphere of Venus ($SO_2$, aerosols, cloud structure). J Geophys Res 1996;101:12709–46.
[3] Barker ES. Detection of $SO_2$ in the UV spectrum of Venus. Geophys Res Lett 1979;6:117–20.
[4] Esposito LW, Copley M, Eckert R, Gates L, Stewart AIF, Worden H. Sulfur dioxide at the Venus cloud tops, 1978–1986. J Geophys Res 1988;93:5267–76.
[5] Esposito LW, Winick JR, Stewart AI. Sulfur dioxide in the Venus atmosphere: distribution and implications. Geophys Res Lett 1979;6:601–4.
[6] Jessup KL, Spencer J, Yelle R. Sulfur volcanism on Io. Icarus 2007;192:24–40.
[7] Bertaux JL, Belton MJS. Evidence of $SO_2$ on Io from UV observations. Nature 1979;282:813–5.
[8] Ballester GE, Mcgrath MA, Strobel DF, Zhu X, Feldman PD, Moos HW. Detection of the $SO_2$ atmosphere on Io with the hubble space telescope. Icarus 1994;111:2–17.
[9] McGrath MA, Belton M, Spencer J, Sartoretti P. Spatially resolved spectroscopy of Io's pele plume and $SO_2$ atmosphere. Icarus 2000;146:476–93.
[10] Kim SJ, A'Hearn MF. Upper limits of SO and $SO_2$ in Comets. Icarus 1991;90:79–95.
[11] Kim SJ, Bockelée-Morvan D, Crovisier J, Biver N. Abundances of SO and $SO_2$ in Comet Hale-Bopp (C/1995 O1). Earth Moon Planets 1997;78:65–6.
[12] Despois D. Radio line observations of molecular and isotopic species in Comet C/1995 O1 (Hale-Bopp). Earth Moon Planets 1997;79:103–24.
[13] Bockelée-Morvan D, Crovisier J. Lessons of Comet Hale-Bopp for coma chemistry: observations and theory. Earth Moon Planets 2002;89:53–71.
[14] Camy-Peyret C, Bergquist B, Galle B, Carleer M, Clerbaux C, Colin R, et al. Intercomparison of instruments for tropospheric measurements using differential optical absorption spectroscopy. J Atm Chem 1996;23:51–80.
[15] Möhler O, Arnold F. Gaseous sulfuric acid and sulfur dioxide measurements in the arctic troposphere and lower stratosphere: implications for hydroxyl radical abundances. Geophys Res Lett 1992;19:1763–6.
[16] Vandaele AC, Tsouli A, Carleer M, Colin R. UV Fourier transform measurements of tropospheric $O_3$, $NO_2$, $SO_2$, benzene, and toluene. Environ Pollut 2002;116:193–201.
[17] Sagawa E, Itoh T. Mass spectrometric observation of $SO_2$ in the stratosphere. Geophys Res Lett 1977;4:29–32.
[18] Jaeschke W, Schmitt R, Georgii H-W. Preliminary results of stratospheric $SO_2$-measurements. Geophys Res Lett 1976;3:517–9.
[19] Carn SA, Krueger AJ, Arellano S, Krotkov NA, Yang K. Daily monitoring of Ecuadorian volcanic degassing from space. J Volcanol Geothermal Res 2008; doi:10.1016/j.jvolgeores.2008.01.029.
[20] Krueger AJ. Sighting of El chichón sulfur dioxide clouds with the Nimbus 7 total ozone mapping spectrometer. Science 1983;220:1377–9.
[21] Krueger AJ, Walter LS, Bhartia PK, Schnetzler CC, Krotkov NA, Sprod I. Volcanic sulfur dioxide measurements from the total ozone mapping spectrometer instruments. J Geophys Res 1995;100:14057–76.
[22] Loyola D, van Geffen J, Valks P, Erbertseder T, Van Roozendael M, Thomas W, et al. Satellite-based detection of volcanic sulphur dioxide from recent eruptions in central and South America. Adv Geosci 2008;14:35–40.
[23] Thomas W, Erbertseder T, Ruppert T, Van Roozendael M, Verdebout J, et al. On the retrieval of volcanic sulfur dioxide emissions from GOME backscatter measurements. J Atm Chem 2004;50:295–320.
[24] Yang K, Krotkov NA, Krueger AJ, Carn SA, Bhartia PK, Levelt PF. Retrieval of large volcanic $SO_2$ columns from the aura ozone monitoring instrument: comparison and limitations. J Geophys Res 2007;112:1.
[25] Eisinger M, Burrows JP. Tropospheric sulfur dioxide observed by the ERS-2 GOME instrument. Geophys Res Lett 1998;25:4177–80.
[26] Hamada Y, Merer AJ. Rotational structure at the long wavelength end of the 2900 Å system of $SO_2$. Can J Phys 1974;52:1443–57.
[27] Hillier IH, Saunders VR. A theoretical interpretation of the bonding, and the photoelectron and ultra-violet spectra of sulphur dioxide. Mol Phys 1971;22:193–201.
[28] Brand JCD, Hardwick JL, Humphrey DR, Hamada Y, Merer AJ. Zeeman effects in the $A^1A_2 \leftarrow X^1A_1$ band system of sulfur dioxide. Can J Phys 1976;54:186–96.
[29] Brand J, Jones V, Di Lauro C. The $^3B_1–^1A_1$ 3880 Å band system of sulfur dioxide: rotational analysis of the 0–0 band. J Mol Spectrosc 1971;40:616–41.
[30] Brand J, Jones V, Di Lauro C. The $^3B_1–^1A_1$ band system of sulfur dioxide: rotational analysis of the (0 1 0), (1 0 0), and (1 1 0) bands. J Mol Spectrosc 1973;45:404–11.
[31] Brand J, Nanes R. The 3000–3400 Å absorption of sulfur dioxide. J Mol Spectrosc 1973;46:194–9.
[32] Hochstrasser RM, Marchetti AP. The spectra of solid SO2 in the $^3B_1–^1A_1$ region. J Mol Spectrosc 1970;35:335–44.
[33] Al-Adel F, Hamdan A, Binbrek O, Baskin JS. Vibrational structure in the low energy region of the $^1A_2$ state of $SO_2$. Chem. Phys. Lett. 1992;189:23–7.
[34] Joens JA. Alternative assignments for the vibrational structure of the $^3B_1–X^1A_1$ band system of $SO_2$. Chem Phys Lett 1996;261:659–64.
[35] Baskin J, Al-Adel F, Hamdan A. Unexpectedly rich vibronic structure in supersonic jet spectra of sulfur dioxide between 360 and 308 nm. Chem Phys Lett 1995;200:181–99.
[36] Huang C-L, Ju S-S, Chen I-C, Merer AJ, Ni C-K, Kung AH. High-resolution spectroscopy of jet-cooled $^{32}SO_2$ and $^{34}SO_2$: The $a\sim^3B_1–X\sim^1A_1$, $2_0^1$ and $1_0^1$ bands. J Mol Spectrosc 2000;203:151–7.
[37] Gerstenkorn S, Luc P. Absolute iodine ($I_2$) standards measured by means of Fourier transform spectroscopy. Rev Phys Appl 1979;14:791–4.
[38] Gerstenkorn S, Luc P. Atlas du spectre d'absorption de la molécule d'iode. France: Editions du CNRS; 1978.
[39] Edlén B. The refractive index of air. Metrologia 1966;2:71–80.
[40] Vandaele AC, Hermans C, Fally S, Carleer M, Mérienne M-F, Jenouvrier A, et al. Absorption cross-section of $NO_2$: simulation of the temperature and pressure effects. J Quant Spectrosc Radiat Transfer 2003;76:373–91.
[41] Vandaele AC, Hermans C, Fally S, Carleer M, Colin R, Mérienne M-F, et al. High-resolution Fourier transform measurement of the $NO_2$ visible and near-infrared absorption cross-sections: temperature and pressure effects. J Geophys Res 2002;107.
[42] Sidebottom HW, Badcock CC, Jackson GE, Calvert JG, Reinhardt GW, Damon EK. Photooxidation of sulfur dioxide. Environ Sci Technol 1972;6:72–9.
[43] Manatt SL, Lane AL. A compilation of the absorption cross-sections of $SO_2$ from 106 to 403 nm. J Quant Spectrosc Radiat Transfer 1993;50:267–76.
[44] Clements JH. On the absorption spectrum of sulphur dioxide. Phys Rev 1933;47:224–32.
[45] Sprague KE, Joens JA. $SO_2$ absorption cross-section measurements from 320 to 405 N m. J Quant Spectrosc Radiat Transfer 1995;53:349–52.
[46] Vandaele AC, Simon PC, Guilmot JM, Carleer M, Colin R. $SO_2$ Absorption cross-section measurement in the UV using a Fourier transform spectrometer. J Geophys Res 1994;99:25599–605.
[47] Sidebottom HW, Badcock CC, Calvert JG, Rheinhardt GW, Rabe BR, Daman EK. A Study of the decay processes in the triplet sulfur dioxide molecule excited at 3828.8 Å. J Am Chem Soc 1971;93:2587–93.